Experimental and Molecular Pathology 108 (2019) 17–23

Contents lists available at ScienceDirect

Experimental and Molecular Pathology

journal homepage: www.elsevier.com/locate/yexmp

Ginsenoside Rh2 inhibits proliferation but promotes apoptosis and autophagy by down-regulating microRNA-638 in human retinoblastoma cells

Man Li, Duzhen Zhang, Jintao Cheng, Jiamei Liang, Fenghua Yu*

Department of Ophtalmology, Linyi Central Hospital, Linyi, Shandong 276400, China

ARTICLE INFO

Keywords:
Retinoblastoma
Ginsenoside Rh2
miR-638
Proliferation
Apoptosis
Autophagy
PI3K/AKT/mTOR

ABSTRACT

Even though recent therapeutic advances make retinoblastoma (RB) becomes a curable tumor, the outcome of long-term survival is poor due to the risk of developing secondary tumors. We aimed to explore the functional role of Ginsenoside Rh2 (GRh2) in human RB cells and the underlying mechanisms. Human RB Y79 and RBL-13 cells were incubated with or without GRh2, followed by assessments of cell viability, proliferation and apoptosis using Cell Counting Kit-8, bromodeoxyuridine, and flow cytometry assays. Meanwhile, expression levels of proteins associated with cell cycle, apoptosis, autophagy and the phosphatidylinositol-3-kinase (PI3K)/AKT/mechanistic target of rapamycin (mTOR) pathway as well as p53 were measured by Western blot analysis. The mRNA expression of cyclinD1, autophagy-related gene 7 (ATG7) and p53, and microRNA (miR)-638 expression were analyzed using quantitative reverse transcription PCR. Then, miR-638 was overexpressed in Y79 and RBL-13 cells followed by treatment with GRh2, and p53 and proteins involved in the PI3K/AKT/mTOR pathway were assessed. Results showed that Y79 and RBL-13 cells viabilities were significantly reduced by 20–50 μM GRh2. Cell proliferation was decreased, and cell apoptosis and autophagy were promoted by 30 μM GRh2 in Y79 and RBL-13 cells. GRh2 decreased miR-638 expression, up-regulated p53 expression, and reduced phosphorylated levels of PI3K, AKT and mTOR. More experiments showed GRh2-induced alterations of p53, phospho (p)-PI3K, p-AKT and p-mTOR were all reversed by miR-638 overexpression. The observations demonstrated that GRh2 functioned in cell proliferation, apoptosis and autophagy in Y79 and RBL-13 cells through miR-638-mediated up-regulation of p53 and inactivation of the PI3K/AKT/mTOR pathway.

1. Introduction

Retinoblastoma (RB) is the most common pediatric intraocular tumor that children below the age of five years are frequently encountered (Kalsoom et al., 2015). Either bilateral or unilateral, one case of every 15,000 to 18,000 live births are diagnosed with RB (Sradhanjali et al., 2017). Clinical symptoms of RB include abnormal whitish appearance of the pupil or leukocoria and strabismus (Kalsoom et al., 2015; Shields and Augsburger, 1981). The current treatments for RB are combined therapeutic strategies of cryotherapies, chemotherapies and laser-based therapies (Rodriguez-Galindo et al., 2003). However, the outcome of severe or late-stage RB remains poor, resulting in enucleation or fatality (Chu et al., 2016). Therefore, innovate and effective therapeutic strategies are pressingly needed.

Ginsenosides, major active chemical ingredients in ginseng, are extracted from the root of *Panax ginseng* Meyer (Jia and Zhao, 2009). Ginsenoside Rh2 (GRh2) is a triterpene saponin, exerting strong anti-inflammatory, anti-diabetic and anti-tumor activities (Song et al., 2017). For instance, proliferation of colon cancer cells has been reported to be repressed by GRh2 (Yang et al., 2016a). In human leukemia Jurkat cells, cell proliferation was inhibited and apoptosis was induced by GRh2 (Xia et al., 2017). Additionally, GRh2 is also reported to repress hepatocellular carcinoma via a coordination of autophagy and the β-catenin signaling (Yang et al., 2016b). However, the functional role of GRh2 in RB cells and the regulatory mechanisms remain unclear.

MicroRNAs (miRNAs/miRs) are small, non-protein-coding, regulatory RNAs that posttranscriptionally modulate gene expression (Kitade et al., 2017). Numerous miRNAs participate in the anti-cancer activity of GRh2 in cancer. A previous literature proved that glioma cell proliferation was inhibited by GRh2 partially via up-regulating miR-128 (Wu et al., 2011). More recently, anti-tumor activity of GRh2 in

* Corresponding author at: Department of Ophtalmology, Linyi Central Hospital, No.17, Jiankang Road, Yishui County, Linyi, Shandong 276400, China.
E-mail address: fenghuayu100@sina.com (F. Yu).

https://doi.org/10.1016/j.yexmp.2019.03.004
Received 26 July 2018; Received in revised form 15 February 2019; Accepted 6 March 2019
Available online 07 March 2019
0014-4800/

hepatitis B virus-related hepatocellular carcinoma was enhanced through up-regulating miR-491 (Chen and Qiu, 2015). Therefore, the interactions between GRh2 and miRNAs are potential regulatory mechanisms that may exist in cancer cells. A literature performed in colorectal cancer cells reported that apoptosis and death were induced by GRh2 via p53 activation (Li et al., 2011). Another literature also reported that cell apoptosis and autophagy, mediated by p53, were promoted by miR-638 knockdown in melanoma cells (Bhattacharya et al., 2015). Thus, a hypothesis that GRh2 functions through miR-638/p53 axis is waiting for systematic investigation.

In our study, the functional roles of GRh2 in cell proliferation, apoptosis and autophagy of human RB Y79 and RBL-13 cells were firstly explored. Moreover, whether GRh2 affected RB cells through miR-638/p53 axis as well as the involved signaling cascades was further verified. Our study aimed to explore effective drug for RB treatment and the underlying mechanisms.

2. Materials and methods

2.1. Cell culture and treatment

The normal retinal miller cells purchased from Meiyan Biotechnology (China) were cultured with L-glutamine and sodium pyruvate in Dulbecco's Modified Eagle's medium (DMEM; Life Technologies, Gaithersburg, MD, USA) with supplementation of 12% inactivated fetal bovine serum (FBS, Gibco, Grand Island, NY, USA), 100 U/mL penicillin, and 100 mg/mL streptomycin at 37 °C and 5% CO_2. Human RB cell lines Y79 and RBL-13 were purchased from American Type Culture Collection (ATCC; Manassas, VA, USA). RB Y79 and RBL-13 cells were maintained in ATCC-formulated RPMI-1640 medium (ATCC) supplemented with 20% fetal bovine serum (FBS; Gibco). Cells were seeded in 25-cm^2 culture flasks and cell culture was performed in a humidified incubator at 37 °C with 5% CO_2. For GRh2 stimulation, Y79 and RBL-13 cells were grown in RPMI-1640 medium containing GRh2 (0–50 μM; Beina Chuanglian Biotechnology Institute, Beijing, China) for 48 h. LY294002 (PI3K inhibitor, 10 μM, Sigma, St Louis, MO, USA) was used to stimulate RBL-13 cells for 24 h in the subsequent experiments.

2.2. Cell counting Kit-8 (CCK-8) assay

Cell viability was measured by using CCK-8 assay. In brief, 5×10^3 normal retinal miller cells, Y79 and RBL-13 cells were plated into each well of 96-well plates, followed by maintaining at 37 °C overnight. Then, culture medium was changed by 100 μL RPMI-1640 medium containing 0, 10, 20, 30, 40 or 50 μM GRh2, and cells were maintained for 48 h at 37 °C. Subsequently, 10 μL CCK-8 solution (Dojindo Molecular Technologies, Inc., Kumamoto, Japan) was added into each well and the cells were incubated at 37 °C for additional 1 h. The absorbance at 450 nm was read using a Microplate Reader (Bio-Rad, Hercules, CA, USA).

2.3. Bromodeoxyuridine (BrdU) assay

Cell proliferation was assessed using a BrdU Cell Proliferation ELISA Kit (Abcam, Cambridge, UK). In brief, Y79 and RBL-13 cells (1×10^5 cells/well) were plated into 96-well plates and incubated at 37 °C overnight. Then, culture medium was changed by 100 μL RPMI-1640 medium with or without GRh2 (30 μM), followed by incubation at 37 °C for 48 h. The BrdU label (20 μL) was added into each well 3 h prior to the end of the incubation period. After centrifugation, the cell pellets were treated with Fixing Solution, anti-BrdU monoclonal Detector Antibody, peroxidase-conjugated goat anti-mouse IgG and TMB Peroxidase substrate in turns on the basis of the manufacturer's protocol. Absorbance was measured at 450/550 nm after addition of Stop Solution using a Microplate Reader (Bio-Rad). The color of positive cells was bright yellow.

2.4. Apoptosis assay

Cell apoptosis was measured by using double-staining with Annexin V-FITC and propidium iodide (PI). Briefly, after stimulation with 30 μM GRh2, 1×10^5 Y79 and RBL-13 cells were washed and stained with Annexin V-FITC and PI following the recommendation of the FITC Annexin V apoptosis detection kit (BD Biosciences, Franklin Lakes, NJ, USA). Subsequently, after being suspended in binding buffer, cells were subjected into a FACS can (Beckman Coulter, Fullerton, CA, USA) for flow cytometry analysis. Percentage of apoptotic cells were analyzed by using FlowJo software (Tree Star, San Carlos, CA, USA).

2.5. Cell transfection

Scramble miRNAs and miR-638 mimic, synthesized by GenePharma Co. (Shanghai, China), were respectively transfected into Y79 and RBL-13 cells using Lipofectamine 3000 reagent (Invitrogen, Carlsbad, CA, USA) according to manufacturer's protocol.

2.6. Quantitative reverse transcription PCR (qRT-PCR)

Total RNA of treated cells was extracted using the TRIzol reagent (Invitrogen) and ethanol precipitation. After quantification using a Nanodrop 2000 system, 500 ng RNA from cells was reversely transcribed to cDNA using the Taqman MicroRNA Reverse Transcription Kit and Multiscribe RT kit (both Applied Biosystems, Foster City, CA, USA) following the suggested procedures for assays of miR-638 and mRNAs, respectively. Then, 50 ng cDNA was acted as template for Quantitative PCR using the Taqman Universal Master Mix II and SYBR Green PCR Master Mix (both Applied Biosystems) according to the manufacturers' protocol for assays of miR-638 and mRNA levels, respectively. The relative expressions of miR-638 and p53 mRNA were calculated using the $2^{-\Delta\Delta Ct}$ method (Livak and Schmittgen, 2001), normalizing to U6 (miR-638) or β-actin (mRNAs).

2.7. Western blot analysis

Cell pellets were lysed using RIPA buffer (Beyotime, Shanghai, China) containing a cocktail of protease inhibitors (Roche, San Francisco, CA, USA). Proteins in the supernatants of lysates were quantified using the BCA™ Protein Assay Kit (Pierce, Appleton, WI, USA). Equivalent proteins were loaded and separated by SDS-PAGE, and the proteins in the gels were transferred to polyvinylidene difluoride (PVDF) membranes. After blocking with 5% non-fat milk, membranes were incubated with respective primary antibody at 4 °C overnight. Antibodies targeting cyclinD1 (ab134175), mammalian B cell lymphoma-2 (Bcl-2; ab196495), Bcl-2-associated X protein (Bax; ab32503), pro caspase-3 (ab44976), cleaved caspase-3 (ab2302), pro caspase-9 (ab2013), cleaved caspase-9 (ab2324), microtubule-associated protein 1 light chain-3 (LC3; ab48394), Beclin-1 (ab62557), p62/sequestosome 1 (p62; ab155686), p53 (ab179477), PI3K (ab135952), phospho (p)-PI3K (ab182651), β-actin (ab8229; all Abcam, Cambridge, UK), autophagy-related gene 7 (ATG7; 8558), AKT (9272), p-AKT (9271), mTOR (2972) or p-mTOR (2971, all Cell Signaling Technology, Beverly, MA, USA) were used in our study. Subsequently, membranes were incubated with secondary antibody marked by horseradish peroxidase (goat anti-rabbit, ab205718, Abcam) for 1 h at room temperature. Proteins in the membranes were visualized by using a SuperSignal West Pico chemiluminescence ECL kit (Pierce).

2.8. Statistical analysis

All experiments were repeated three times. The results were presented as the mean ± standard deviation (SD). Statistical analysis was

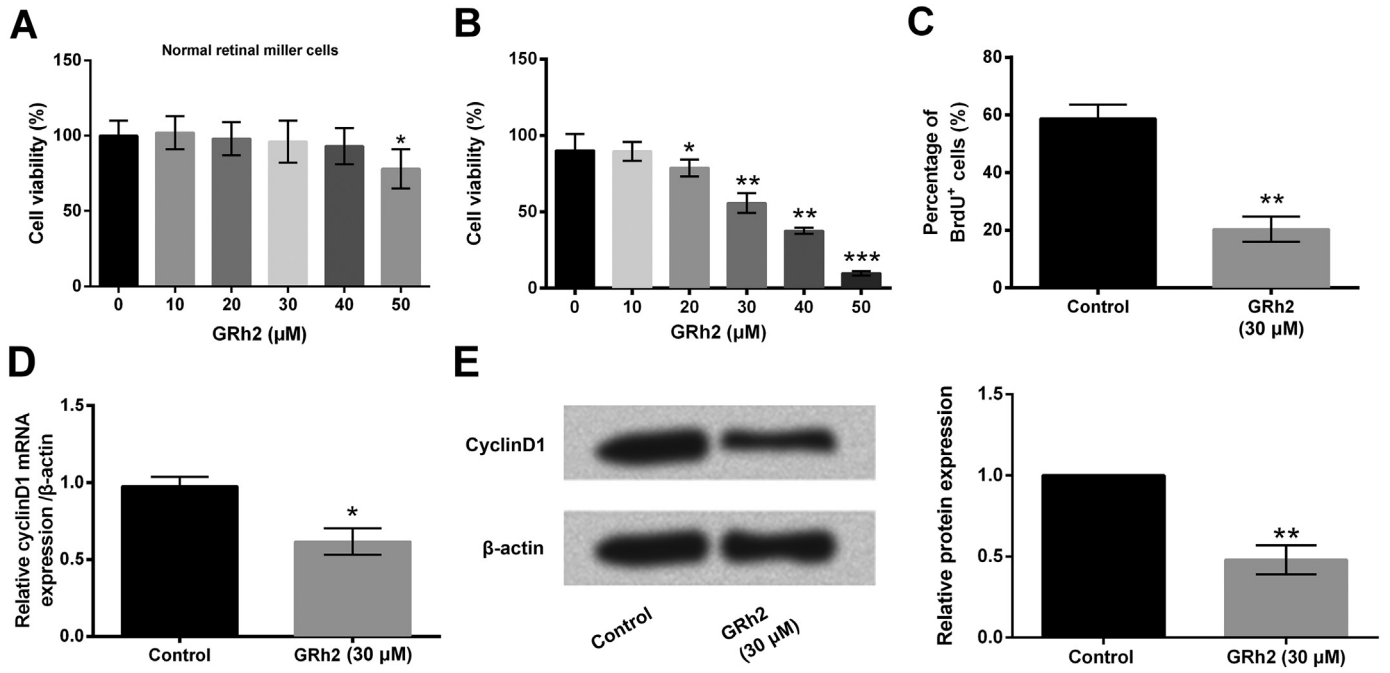

Fig. 1. Ginsenoside Rh2 (GRh2) inhibits retinoblastoma Y79 cell proliferation. A. Different doses of GRh2 (0–50 μM) were used to treat normal retinal miller cells, and cell viability by Cell Counting Kit-8 assay. Different doses of GRh2 were used to treat Y79 cells. Non-treated cells were acted as control. B. Cell viability by Cell Counting Kit-8 assay. C. Percentage of Bromodeoxyuridine (BrdU) positive cells by BrdU assay. D. and E. mRNA and protein expressions of cyclinD1 by quantitative reverse transcription PCR and Western blot analysis, respectively. Data are presented as means ± SD. *, $P < 0.05$; **, $P < 0.01$; ***, $P < 0.001$.

performed using Graphpad Prism 5 software (GraphPad, San Diego, CA, USA). The *P*-values were calculated using the unpaired two-tailed *t*-test or one-way analysis of variance (ANOVA). A $P < 0.05$ was considered as a significant difference.

3. Results

3.1. GRh2 inhibits RB cells proliferation

In this study, we performed a preliminary experiment to observe the cell cytotoxicity of GRh2 on normal retinal miller cells. The different doses of GRh2 (0–50 μM) were used to treat normal retinal miller cells, and cell viability was examined. The results showed that 50 μM GRh2 was significantly reduced cell viability of normal retinal miller cells ($P < 0.05$, Fig. 1A). Concentration of GRh2 at 10–40 μM had no effect on cell viability (Fig. 1A). These data indicated that GRh2 at 50 μM of GRh2 had toxic to normal retinal miller cells. Subsequently, RB cell line Y79 was stimulated with diverse doses of GRh2 and cell viability was measured. Compared with cells treated with 0 μM GRh2, cell viability was significantly reduced by 20 μM ($P < 0.05$), 30 μM, 40 μM (both $P < 0.01$) and 50 μM ($P < 0.001$) of GRh2 (Fig. 1B). However, the effect of 10 μM GRh2 on cell viability was non-significant. Due to the IC50 for cell viability was nearly 30 μM of GRh2, thus, 30 μM of GRh2 was used for the further experiments. Then, in Fig. 1C, the percentage of BrdU positive cells in the GRh2 group was markedly lower than that in the control group ($P < 0.01$). Meanwhile, mRNA and protein levels of cyclinD1 were dramatically down-regulated after stimulation of GRh2 as compared to the control group ($P < 0.05$, Fig. 1D and E). Other RB cell line RBL-13, was also treated with the different concentrations of GRh2 (0–50 μM). We observed that cell viability was significantly decreased by GRh2 in a dose dependent manner ($P < 0.05$, $P < 0.01$ or $P < 0.001$, Supplementary Fig. 1A). Then, 30 μM GRh2 was selected for stimulating RBL-13 cells in the following experiments. Next, cells were treated with 30 μM GRh2 or 10 μM LY294002 (PI3K inhibitor). The results showed that the percentage of BrdU positive cells was reduced by GRh2 and LY294002 ($P < 0.01$, Supplementary Fig. 1B). Additionally, the mRNA and protein levels of CyclinD1 were all decreased by GRh2 and LY294002 ($P < 0.05$, Supplementary Fig. 1C and D). Taken together, we concluded that GRh2 could inhibit RB cells proliferation.

3.2. GRh2 promotes RB cell apoptosis

After stimulation with GRh2, alterations of apoptotic Y79 cells and apoptosis-related proteins were assessed. As shown in Fig. 2A, percentage of apoptotic cells in the GRh2 group was significantly higher than that in the control group ($P < 0.01$). Likewise, expression of Bcl-2 (anti-apoptosis) was down-regulated whereas expressions of Bax, cleaved caspase-3 and cleaved caspase-9 (pro-apoptosis) were all up-regulated by GRh2 stimulation ($P < 0.05$ or $P < 0.01$, Fig. 2B). Similarly, cell apoptosis were all induced in GRh2 or LY294002 treated cells ($P < 0.001$, Supplementary Fig. 2A). The protein level of Bcl-2 was down-regulated, but protein levels of Bax, cleaved caspase-3 and cleaved caspase-9 were all up-regulated in GRh2 or LY294002 treated cells ($P < 0.05$, $P < 0.01$ or $P < 0.001$, Supplementary Fig. 2B). Data showed GRh2 promoted cell apoptosis in Y79 and RBL-13 cells.

3.3. GRh2 promotes RB cell autophagy

To assess the effects of GRh2 on Y79 cell autophagy, expressions of autophagy-related proteins were tested. Compared with the control group, mRNA and protein expressions of ATG7 were both markedly up-regulated by GRh2 ($P < 0.05$; Fig. 3A and B). More data in Fig. 3C showed that the ratios of LC3-II/I and Beclin-1 level were increased while p62 level was reduced after stimulation of GRh2. The effects of GRh2 and LY294002 on RBL-13 cell autophagy were also investigated. We observed that mRNA and protein expressions of ATG7 were all up-regulated by LY294002 and GRh2 ($P < 0.05$ or $P < 0.01$, Supplementary Fig. 3A and B). Results in Supplementary Fig. 3C showed that the ratios of LC3-II/I and Beclin-1 levels were increased but p62 level was reduced after treatment with LY294002 or GRh2 ($P < 0.05$ or $P < 0.01$). Those results illustrated that GRh2 could promote Y79 and

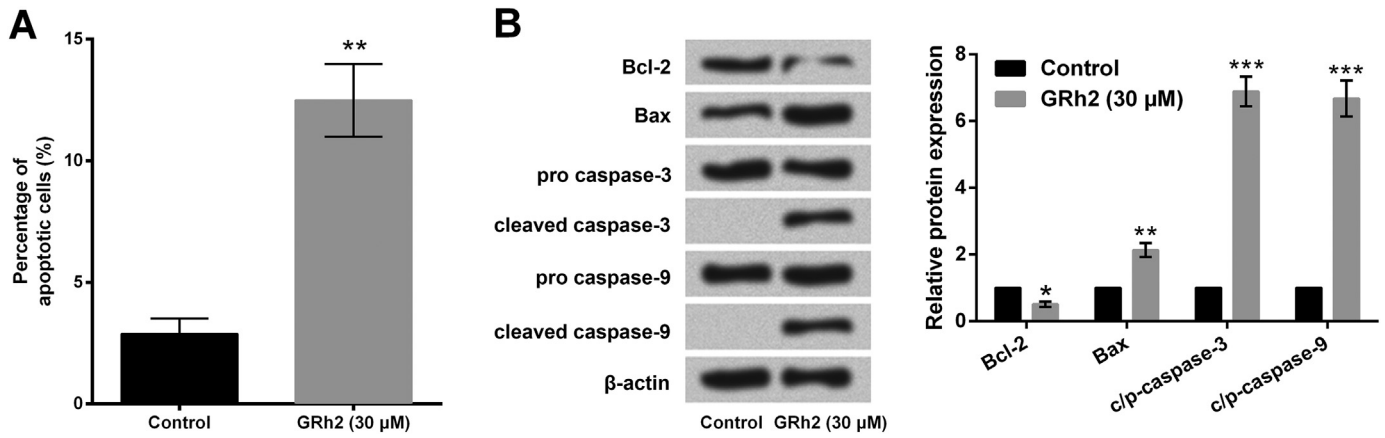

Fig. 2. Ginsenoside Rh2 (GRh2) promotes retinoblastoma Y79 cell apoptosis. Non-treated cells were acted as control. A. Percentage of apoptotic cells by flow cytometry assay. B. Expression of apoptosis-associated proteins by Western blot analysis. Data are presented as mean ± SD. *, $P < 0.05$; **, $P < 0.01$, ***, $P < 0.001$.

RBL-13 cell autophagy.

3.4. GRh2 down-regulates miR-638 in Y79 and RBL-13 cells

To figure out the underlying mechanism of GRh2-associated regulation, expression level of miR-638 after GRh2 stimulation in Y79 cells was assessed. In Fig. 4, miR-638 level in the GRh2 group was significantly lower than that in the control group ($P < 0.01$). Similarly, the expression level of miR-638 was also reduced in RBL-13 cells after LY294002 or GRh2 stimulation ($P < 0.01$, Supplementary Fig. 4). Data suggested that GRh2 could down-regulate expression of miR-638 in Y79 and RBL-13 cells.

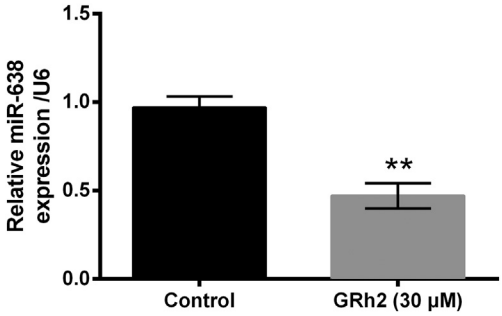

Fig. 4. Ginsenoside Rh2 (GRh2) down-regulates microRNA (miR)-638 in retinoblastoma Y79 cells. Non-treated cells were acted as control. miR-638 level was by measured by quantitative reverse transcription PCR. Data are presented as mean ± SD. **, $P < 0.01$.

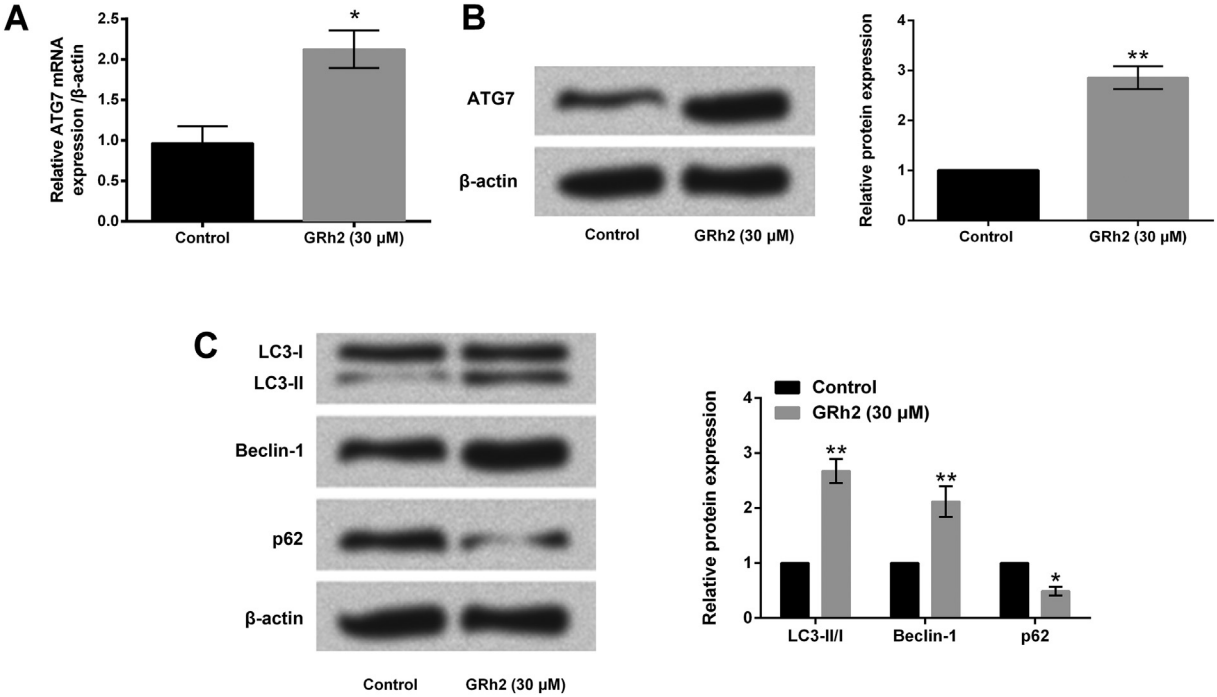

Fig. 3. Ginsenoside Rh2 (GRh2) promotes retinoblastoma Y79 cell autophagy. Non-treated cells were acted as control. A. and B. mRNA and protein expressions of autophagy-related gene 7 (ATG7) by quantitative reverse transcription PCR and Western blot analysis, respectively. C. Expressions of autophagy-related proteins by Western blot analysis. Data are presented as mean ± SD. *, $P < 0.05$; **, $P < 0.01$. LC, microtubule-associated protein 1 light chain-3; p62, p62/sequestosome 1.

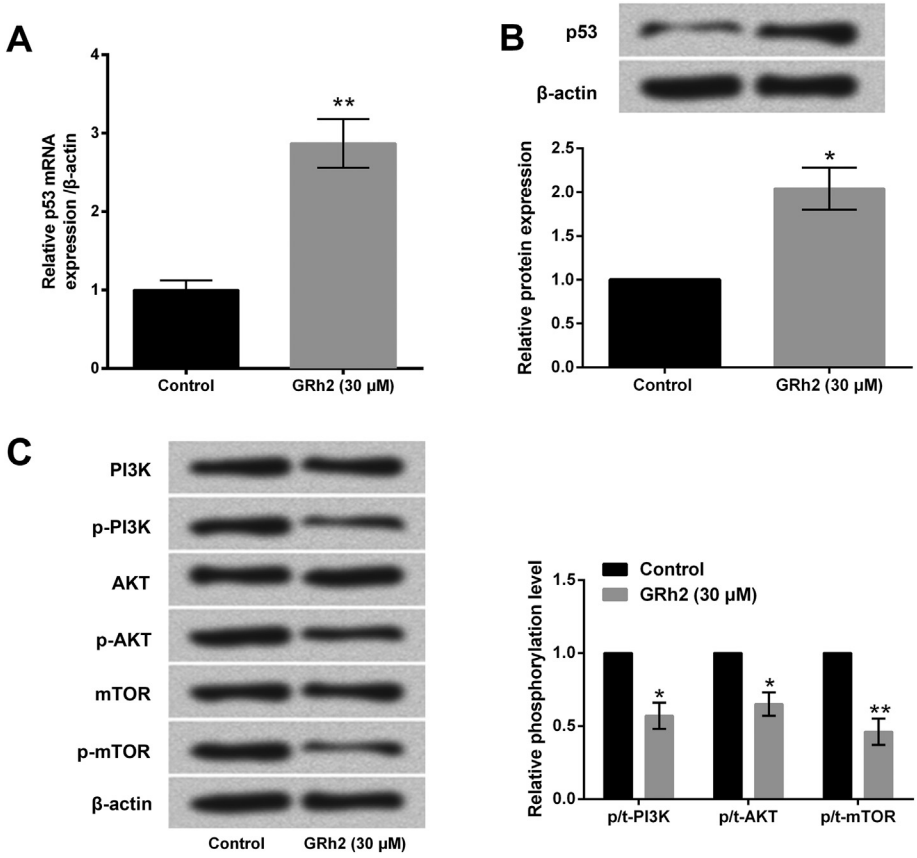

Fig. 5. Ginsenoside Rh2 (GRh2) up-regulates p53 and inhibits the PI3K/AKT/mTOR pathway in retinoblastoma Y79 cells. Non-treated cells were acted as control. A. and B. mRNA and protein expressions of p53 by quantitative reverse transcription PCR and Western blot analysis, respectively. C. Expressions of key kinases in the PI3K/AKT/mTOR pathway by Western blot analysis. Data are presented as mean ± SD. *, $P < 0.05$; **, $P < 0.01$. PI3K, phosphatidylinositol-3-kinase; mTOR, mechanistic target of rapamycin; p-, phospho-.

3.5. GRh2 up-regulates p53 and inactivates the PI3K/AKT/mTOR pathway in Y79 cells and RBL-13 cells

To explore the underlying mechanisms, expressions of p53 and key kinases in the PI3K/AKT/mTOR pathway were also assessed. Compared with the control group, mRNA and protein expressions of p53 were both up-regulated by GRh2 ($P < 0.05$ or $P < 0.01$; Fig. 5A and B). Conversely, phosphorylated levels of PI3K, AKT and mTOR were all obviously reduced by GRh2 ($P < 0.05$ or $P < 0.01$, Fig. 5C). Additionally, increased mRNA and protein levels of p53 were all observed in LY294002 or GRh2 treated RBL-13 cells ($P < 0.05$, $P < 0.01$ or $P < 0.001$; Supplementary Fig. 5A and B). Moreover, the phosphorylated levels of PI3K, AKT and mTOR were all decreased by LY294002 or GRh2 ($P < 0.05$ or $P < 0.01$, Supplementary Fig. 5C). Those results stated that GRh2 up-regulated p53 and inhibited the PI3K/AKT/mTOR pathway in Y79 and RBL-13 cells.

3.6. GRh2 up-regulates p53 and inactivates the PI3K/AKT/mTOR pathway through down-regulating miR-638 in Y79 and RBL-13 cells

After cell transfection, miR-638 level in Y79 cells transfected with miR-638 mimic was dramatically higher than that in cells transfected with scramble miRNAs ($P < 0.01$; Fig. 6A), indicating that miR-638 was successfully overexpressed after cell transfection. Then, transfected Y79 cells were incubated with GRh2, followed by further analysis the expression level of miR-638. In Fig. 6B, miR-638 overexpression reversed the down-regulatory effect of GRh2 on miR-638 expression ($P < 0.001$). In Fig. 6C and D, up-regulation of p53 and down-regulations of p-PI3K, p-AKT and p-mTOR, induced by GRh2, were all reversed by miR-638 overexpression ($P < 0.05$ or $P < 0.01$). Further, the down-regulatory effect of GRh2 on Bcl-2 and the up-regulatory effect of GRh2 on Bax, cleaved caspase-3 and cleaved caspase-9 were all reversed by miR-638 overexpression ($P < 0.05$, $P < 0.01$ or $P < 0.001$, Fig. 6E and F). In RBL-13 cells, we observed that GRh2 notably up-regulated p53 expression and down-regulated p-PI3K, p-AKT and p-mTOR expressions ($P < 0.05$ or $P < 0.01$). MiR-638 overexpression showed opposite results ($P < .05$). After treatment with LY294002, the regulatory effects of miR-638 overexpression on p53 and PI3K/AKT/mTOR pathway were also reversed ($P < 0.05$ or $P < 0.01$, Supplementary Fig. 6). Results illustrated that GRh2 up-regulated p53 and inhibited the PI3K/AKT/mTOR pathway through down-regulating miR-638 in Y79 and RBL-13 cells.

4. Discussion

Even though recent therapeutic advances make RB become a curable tumor, the risk of developing secondary tumors leads to reduction of long-term survival (Aerts et al., 2016). Hence, more effective therapeutic strategies for RB are challenging. In our study, GRh2 was firstly identified to repress cell proliferation and induce apoptosis and autophagy in RB Y79 and RBL-13 cells. More experiments proved that GRh2 functioned in Y79 and RBL-13 cells through miR-638-mediated up-regulation of p53 and inhibition of the PI3K/AKT/mTOR pathway.

RB results from the inactivation of the *RB1* gene, which is located on chromosome 13q14 and widely reported as a tumor suppressor gene (Friend et al., 1986). The nuclear phosphoprotein pRB, encoded by *RB1* gene, is a negative regulator of G1 to S phase transition (Castillo-Martin et al., 2010). Therefore, the proliferation in RB cells is non-physiologically increased due to the inactivation of the *RB1* gene. In our study, alteration of cell proliferation after GRh2 treatments in Y79 and RBL-13 cells was firstly tested, showing that cell viability and proliferation of Y79 and RBL-13 cells were both reduced by GRh2. CyclinD1 is a positive regulator of cell cycle progression, which take cell cycle from G1 phase to S phase (Bertoli et al., 2013). The down-regulated cyclinD1 after GRh2 stimulation supported the reduced cell viability and proliferation.

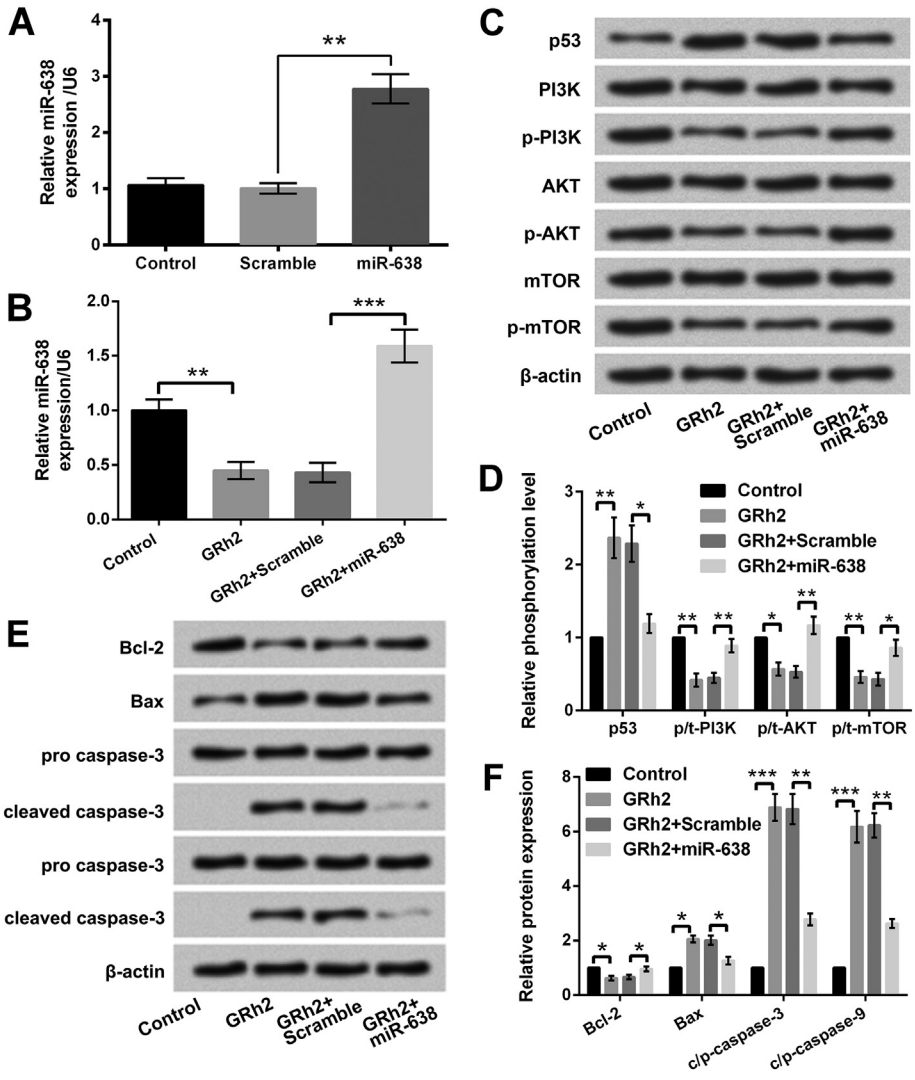

Fig. 6. Ginsenoside Rh2 (GRh2) up-regulates p53 and inhibits the PI3K/AKT/mTOR pathway in retinoblastoma Y79 cells through down-regulating microRNA (miR)-638. A. Y79 cells were transfected with scramble miRNAs or miR-638 mimics (miR-638), expression of miR-638 by quantitative reverse transcription PCR. Y79 cells were transfected with scramble miRNAs or miR-638 mimics, followed by stimulation with GRh2. B. Expression of miR-638 by quantitative reverse transcription PCR. C. and D. Expressions of p53 and key kinases in the PI3K/AKT/mTOR pathway by Western blot analysis. E. and F. Expression of apoptosis-associated proteins by Western blot analysis. Data are presented as mean ± SD. *, $P < 0.05$; **, $P < 0.01$; ***, $P < 0.001$. PI3K, phosphatidylinositol-3-kinase; mTOR, mechanistic target of rapamycin; p-, phospho.

pRB can directly activate mitochondrial apoptosis exerting tumor suppressive function (Hilgendorf et al., 2013). In RB, the inactivation of pRB may lead to blockade of cell apoptosis. In our study, the GRh2 significantly enhanced cell apoptosis in Y79 and RBL-13 cells. Furthermore, the anti-apoptotic Bcl-2 was down-regulated whereas pro-apoptotic Bax was up-regulated after GRh2 stimulation, resulting in increased activation of caspase-9 and caspase-3 in turns. As active caspase-3 is the primary executioner of apoptotic death (Brentnall et al., 2013), the up-regulated active caspase-3 supported the enhanced cell apoptosis after GRh2 stimulation.

Autophagy is a conserved degradation pathway that coordinated with lysosomal (Chen et al., 2016). Like apoptosis, autophagy, is another mechanisms of programmed cell death (Liberski, 2017). Double membrane vesicles termed autophagosomes were formatted during autophagy. ATG7 is a critical factor that participates in the elongation and closure of the autophagosomal membrane (Mizushima et al., 2011). When the autophagy is initiated, LC3-I was lipidated (LC3-II) and bond with autophagosomes (Kabeya et al., 2000). Beclin-1 is also reported as a pivotal factor involved in autophagosome formation (Maejima et al., 2016). P62, which is added to ubiquitinated proteins, is a selective autophagy substrate and can be directly degraded in lysosomal (Kauppinen et al., 2017). In our study, the up-regulated ATG7, LC3-II/I, Beclin-1 and down-regulated p62, induced by GRh2 in both Y79 and RBL-13 cells, illustrated enhanced autophagy which provided supports for the anti-tumor activity of GRh2.

As reported previously, GRh2 induces cell death and apoptosis through p53 activation, and p53-mediated cell apoptosis and autophagy can be increased by miR-638 (Bhattacharya et al., 2015; Li et al., 2011). Thus, we hypothesized that miR-638 might be involved in the anti-tumor activity of GRh2. Accordingly, expression of miR-638 in Y79 and RBL-13 cells was identified to be down-regulated after GRh2 stimulation, suggesting the possible involvements of miR-638. p53 is a nuclear transcription factor that suppresses tumor progress through repressing cell proliferation, and promoting apoptosis and autophagy (Liu et al., 2016; Zhang et al., 2016). The PI3K/AKT/mTOR cascade is a frequently activated pathway in cancer cells that modulates cell metabolism, differentiation, proliferation, apoptosis, and etc. (Polivka and Janku, 2014; Xu et al., 2014). To further explore the regulatory mechanism of GRh2 in Y79 and RBL-13 cells, expression of p53 and activation of the PI3K/AKT/mTOR pathway was measured. Results in our study proved that p53 was up-regulated and the PI3K/AKT/mTOR pathway was inhibited after GRh2, illustrating the involvements of p53 and the PI3K/AKT/mTOR pathway after GRh2 treatments. Combined the GRh2-induced changes including down-regulated miR-638, up-regulated p53 and inactivated PI3K/AKT/mTOR pathway, we finally explored the possible interactions between those altered factors. When miR-638 was overexpressed, the GRh2-induced up-regulation of p53 and inactivation of the PI3K/AKT/mTOR pathway were both reversed. Therefore, we speculated that GRh2 up-regulated p53 and inactivated the PI3K/AKT/mTOR pathway through down-regulating miR-638.

More experiments are still needed for further verification before clinical application of GRh2.

To summarize, GRh2 repressed cell proliferation and induced cell apoptosis and autophagy in RB Y79 and RBL-13 cells. For mechanism study, we interestingly found GRh2 up-regulated p53 and inactivated the PI3K/AKT/mTOR pathway through down-regulating miR-638 in Y79 and RBL-13 cells. This study provides theoretical basis for deeply exploring the role of GRh2 in RB cells, aiding to find innovate therapeutic strategies for treatment of RB in clinical.

Supplementary data to this article can be found online at https://doi.org/10.1016/j.yexmp.2019.03.004.

Competing interests

The authors declare that they have no competing interests.

Acknowledgements

None.

References

Aerts, I., et al., 2016. Retinoblastoma update. Archives de pediatrie : organe officiel de la Societe francaise de pediatrie 23, 112–116.
Bertoli, C., et al., 2013. Control of cell cycle transcription during G1 and S phases. Nat. Rev. Mol. Cell Biol. 14, 518–528.
Bhattacharya, A., et al., 2015. miR-638 promotes melanoma metastasis and protects melanoma cells from apoptosis and autophagy. Oncotarget. 6, 2966–2980.
Brentnall, M., et al., 2013. Caspase-9, caspase-3 and caspase-7 have distinct roles during intrinsic apoptosis. BMC Cell Biol. 14, 32.
Castillo-Martin, M., et al., 2010. Molecular pathways of urothelial development and bladder tumorigenesis. Urol. Oncol. 28, 401–408.
Chen, W., Qiu, Y., 2015. Ginsenoside Rh2 targets EGFR by up-regulation of miR-491 to enhance anti-tumor activity in hepatitis B virus-related hepatocellular carcinoma. Cell Biochem. Biophys. 72, 325–331.
Chen, Y., et al., 2016. Tyrosine kinase receptor EGFR regulates the switch in cancer cells between cell survival and cell death induced by autophagy in hypoxia. Autophagy. 12, 1029–1046.
Chu, W.K., et al., 2016. Antagonists of growth hormone-releasing hormone receptor induce apoptosis specifically in retinoblastoma cells. Proc. Natl. Acad. Sci. U. S. A. 113, 14396–14401.
Friend, S.H., et al., 1986. A human DNA segment with properties of the gene that predisposes to retinoblastoma and osteosarcoma. Nature. 323, 643–646.
Hilgendorf, K.I., et al., 2013. The retinoblastoma protein induces apoptosis directly at the mitochondria. Genes Dev. 27, 1003–1015.
Jia, L., Zhao, Y., 2009. Current evaluation of the millennium phytomedicine–ginseng (I): etymology, pharmacognosy, phytochemistry, market and regulations. Curr. Med. Chem. 16, 2475–2484.
Kabeya, Y., et al., 2000. LC3, a mammalian homologue of yeast Apg8p, is localized in autophagosome membranes after processing. EMBO J. 19, 5720–5728.
Kalsoom, S., et al., 2015. Alterations in the RB1 gene in Pakistani patients with retinoblastoma using direct sequencing analysis. Mol. Vis. 21, 1085–1092.
Kauppinen, A., et al., 2017. The role of p62/SQSTM1 in IL-1β-mediated cytokine production in retinal pigment epithelial cells. Acta Ophthalmol. 95 (n/a-n/a).
Kitade, Y., et al., 2017. Chemical modification of the 3′-dangling end of small interfering RNAs such as siRNAs and miRNAs: The development of miRNA replacement therapy. In: Tomioka, K. (Ed.), New Horizons of Process Chemistry: Scalable Reactions and Technologies. Springer Singapore, Singapore, pp. 237–249.
Li, B., et al., 2011. Ginsenoside Rh2 induces apoptosis and paraptosis-like cell death in colorectal cancer cells through activation of p53. Cancer Lett. 301, 185–192.
Liberski, P.P., 2017. Cell death and autophagy in prion diseases. In: Liberski, P.P. (Ed.), Prion Diseases. Springer New York, New York, NY, pp. 145–158.
Liu, C., et al., 2016. H19-derived miR-675 contributes to bladder cancer cell proliferation by regulating p53 activation. Tumor Biol. 37, 263–270.
Livak, K.J., Schmittgen, T.D., 2001. Analysis of relative gene expression data using real-time quantitative PCR and the 2(− Delta Delta C(T)) method. Methods. 25, 402–408.
Maejima, Y., et al., 2016. Regulation of autophagy by Beclin 1 in the heart. J. Mol. Cell. Cardiol. 95, 19–25.
Mizushima, N., et al., 2011. The role of Atg proteins in Autophagosome formation. Annu. Rev. Cell Dev. Biol. 27, 107–132.
Polivka, J., Janku, F., 2014. Molecular targets for cancer therapy in the PI3K/AKT/mTOR pathway. Pharmacol. Ther. 142, 164–175.
Rodriguez-Galindo, C., et al., 2003. Treatment of metastatic retinoblastoma. Ophthalmology. 110, 1237–1240.
Shields, J.A., Augsburger, J.J., 1981. Current approaches to the diagnosis and management of retinoblastoma. Surv. Ophthalmol. 25, 347–372.
Song, B.-K., et al., 2017. Production of the rare Ginsenoside Rh2-MIX (20(S)-Rh2, 20(R)-Rh2, Rk2, and Rh3) by enzymatic conversion combined with acid treatment and evaluation of its anti-Cancer activity. J. Microbiol. Biotechnol. 27, 1233–1241.
Sradhanjali, S., et al., 2017. Overexpression of pyruvate dehydrogenase kinase 1 in retinoblastoma: A potential therapeutic opportunity for targeting vitreous seeds and hypoxic regions. 12. pp. e0177744.
Wu, N., et al., 2011. Ginsenoside Rh2 inhibits glioma cell proliferation by targeting microRNA-128. Acta Pharmacol. Sin. 32, 345–353.
Xia, T., et al., 2017. Ginsenoside Rh2 and Rg3 inhibit cell proliferation and induce apoptosis by increasing mitochondrial reactive oxygen species in human leukemia Jurkat cells. Mol. Med. Rep. 15, 3591–3598.
Xu, Y., et al., 2014. Emerging roles of the p38 MAPK and PI3K/AKT/mTOR pathways in oncogene-induced senescence. Trends Biochem. Sci. 39, 268–276.
Yang, J., et al., 2016a. Ginsenoside Rh2 inhibiting HCT116 colon cancer cell proliferation through blocking PDZ-binding kinase/T-LAK cell-originated protein kinase. J. Ginseng Res. 40, 400–408.
Yang, Z., et al., 2016b. Ginsenoside Rh2 inhibits hepatocellular carcinoma through β-catenin and autophagy. Sci. Rep. 6, 19383.
Zhang, X., et al., 2016. TRAF6 restricts p53 mitochondrial translocation, apoptosis, and tumor suppression. Mol. Cell 64, 803–814.